Raman and Infrared Spectroscopy of Cyanide-Inhibited CO Dehydrogenase/Acetyl-CoA Synthase from *Clostridium thermoaceticum*: Evidence for Bimetallic Enzymatic CO Oxidation

Di Qiu,[†] Manoj Kumar,[‡] Stephen W. Ragsdale,*[,‡] and Thomas G. Spiro*[,†]

Contribution from the Department of Biochemistry, Beadle Center, University of Nebraska, Lincoln, Nebraska 68588-0664, and Department of Chemistry, Princeton University, Princeton, New Jersey 08544

Received February 12, 1996[⊗]

Abstract: *Clostridium thermoaceticum* and other autotrophic anaerobic bacteria contain a bifunctional enzyme, carbon monoxide dehydrogenase/acetyl-CoA synthase (CODH/ACS), that catalyzes two reactions of CO at two separate Ni−FeS clusters. Oxidation of CO to CO_2 is catalyzed by Cluster C, while incorporation of CO into acetyl-CoA occurs at Cluster A. In this study, resonance Raman [RR] and infrared [IR] spectroscopy are applied to the adduct of Cluster C with cyanide, a selective inhibitor of CO oxidation. The RR spectra reveal that CN^- binds simultaneously to Fe and Ni, because bands whose ^{13}C and ^{15}N shifts identify them as cyanide−metal stretching and bending modes are sensitive to incorporation of both ^{54}Fe and ^{64}Ni into the enzyme. The IR spectrum reveals a low frequency, 2037 cm^{-1}, for the C−N stretch, indicative of Fe^{II} binding via the C end. Vibrational modeling of the frequencies and isotope shifts indicates a bent Fe−CN−Ni bridging geometry, with a ∼140° C−N−Ni angle. This geometry of the inhibitory adduct suggests that CO oxidation involves a bimetallic mechanism. It is proposed that pre-organization of the metal ions by the enzyme promotes CO oxidation by $Ni^{II}-OH^-$ attack on Fe^{II}−CO, followed by Ni−FeS reduction as CO_2 is released. This chemistry is analogous to the metal-catalyzed water-gas shift reaction.

Carbon monoxide dehydrogenase/acetyl-CoA synthase[1] (CODH/ACS) contains 11−14 Fe, 2 Ni, Zn, and 13 S^{2-} per 150-kDa dimer.[2] The metal ions are organized into at least three distinct centers.[3−9] Cluster A, which catalyzes acetyl-CoA synthesis,[10−13] has been identified as a [Ni−X−Fe_4S_4] center (X is an unknown bridging ligand between Ni and Fe) by EPR,[4,7] Mössbauer,[8] and ENDOR[9] studies of the native protein and of the isolated α subunit.[14−16] Cluster C, the site of CO oxidation,[12,17] has likewise been proposed to be a [Ni−X−Fe_4S_4] cluster,[18] while Cluster B, which is involved in electron transfer reactions during CO oxidation,[12] is a typical $[4Fe-4S]^{2+/1+}$ cluster.[7,8] Clusters B and C are present in all the Ni-containing enzymes that perform CO oxidation.[7,18−23] This study focuses on Cluster C and the mechanism of CO oxidation.

In its oxidized state (C_{ox}) Cluster C of CODH/ACS is diamagnetic, while the one-electron reduced state (C_{red1}) exhibits EPR signals with *g* values at 2.01, 1.81, and 1.65. The midpoint potential for this reduction is relatively high, ranging from −35 mV for the *Methanosarcina barkeri* enzyme[20] to −220 mV for the *Clostridium thermoaceticum* protein.[7] The EPR spectrum of Cluster C_{red1} is pH-dependent reflecting an ionization with a pK_a of 7.6.[24] Under more reducing conditions [midpoint potential of −530 mV[7,25]], C_{red1} is replaced by C_{red2}, whose EPR spectrum is characterized by having all *g* values below 2.0 (1.97,

[†] Princeton University.

[‡] University of Nebraska.

[⊗] Abstract published in *Advance ACS Abstracts,* October 1, 1996.

(1) "CO dehydrogenase" (CODH) is the recommended name for the activity that catalyzes CO oxidation to CO_2 or its reverse. "Acetyl-CoA synthase" (ACS) is the recommended name for the activity that assembles acetyl-CoA from enzyme-bound methyl, CO, and CoA groups. The bifunctional enzyme from acetogens and methanogens is designated "CO dehydrogenase/acetyl-CoA synthase" (CODH/ACS); the monofunctional enzyme from *R. rubrum* is denoted CODH [Ragsdale, S. W.; Kumar, M. *Chem. Rev.* In press].

(2) Ragsdale, S. W.; Clark, J. E.; Ljungdahl, L. G.; Lundie, L. L.; Drake, H. L. *J. Biol. Chem.* **1983**, *258*, 2364−2369.

(3) Shin, W.; Stafford, P. R.; Lindahl, P. A. *Biochemistry* **1992**, *31*, 6003−6011.

(4) Ragsdale, S. W.; Wood, H. G.; Antholine, W. E. *Proc. Natl. Acad. Sci. U.S.A.* **1985**, *82*, 6811−6814.

(5) Ragsdale, S. W.; Ljungdahl, L. G.; DerVartanian, D. V. *Biochem. Biophys. Res. Commun.* **1983**, *115*, 658−665.

(6) Ragsdale, S. W.; Ljungdahl, L. G.; DerVartanian, D. V. *Biochem. Biophys. Res. Commun.* **1982**, *108*, 658−663.

(7) Lindahl, P. A.; Münck, E.; Ragsdale, S. W. *J. Biol. Chem.* **1990**, *265*, 3873−3879.

(8) Lindahl, P. A.; Ragsdale, S. W.; Münck, E. *J. Biol. Chem.* **1990**, *265*, 3880−3888.

(9) Fan, C.; Gorst, C. M.; Ragsdale, S. W.; Hoffman, B. M. *Biochemistry* **1991**, *30*, 431−435.

(10) Shin, W.; Lindahl, P. A. *Biochemistry* **1992**, *31*, 12870−12875.

(11) Gorst, C. M.; Ragsdale, S. W. *J. Biol. Chem.* **1991**, *266*, 20687−20693.

(12) Kumar, M.; Lu, W.-P.; Liu, L.; Ragsdale, S. W. *J. Am. Chem. Soc.* **1993**, *115*, 11646−11647.

(13) Qiu, D.; Kumar, M.; Ragsdale, S. W.; Spiro, T. G. *J. Am. Chem. Soc.* **1995**, *117*, 2653−2654.

(14) Xia, J. Q.; Lindahl, P. A. *Biochemistry* **1995**, *34*, 6037−6042.

(15) xia, J. Q.; Dong, J.; Wang, S. K.; Scott, R. A.; Lindahl, P. A. *J. Am. Chem. Soc.* **1995**, *117*, 7065−7070.

(16) Xia, J. Q.; Lindahl, P. A. *J. Am. Chem. Soc.* **1996**, *118*, 483−484.

(17) Anderson, M. E.; DeRose, V. J.; Hoffman, B. M.; Lindahl, P. A. *J. Am. Chem. Soc.* **1993**, *115*, 12204−12205.

(18) Hu, Z. G.; Spangler, N. J.; Anderson, M. E.; Xia, J. Q.; Ludden, P. W.; Lindahl, P. A.; Münck, E. *J. Am. Chem. Soc.* **1996**, *118*, 830−845.

(19) Lu, W.-P.; Jablonski, P. E.; Rasche, M.; Ferry, J. G.; Ragsdale, S. W. *J. Biol. Chem.* **1994**, *269*, 9736−9742.

(20) Krzycki, J. A.; Mortenson, L. E.; Prince, R. C. *J. Biol. Chem.* **1989**, *264*, 7217−7221.

(21) Jetten, M. S. M.; Hagen, W. R.; Pierik, A. J.; Stams, A. J. M.; Zehnder, A. J. B. *Eur. J. Biochem.* **1990**,

(22) Bonam, D.; Ludden, P. W. *J. Biol. Chem.* **1987**, *262*, 2980−2987.

(23) Stephens, P. J.; McKenna, M.-C.; Ensign, S. A.; Bonam, D.; Ludden, P. W. *J. Biol. Chem.* **1989**, *264*, 16347−16350.

(24) Seravalli, J.; Kumar, M.; Lu, W. P.; Ragsdale, S. W. *Biochemistry* **1995**, *34*, 7879−7888.

(25) Spangler, N. J.; Lindahl, P. A.; Bandarian, V.; Ludden, P. *J. Biol. Chem.* In press.

S0002-7863(96)00435-0 CCC: $12.00

1.86, 1.75). Because of uncertainties in quantitation, however, it is not known whether C_{red2} has two more electrons than C_{red1}, or is instead a variant of the cluster which is at the same oxidation level as C_{red1}.

Several anions inhibit the enzyme and alter the spectroscopic properties of Cluster C. Thiocyanate, azide, cyanate, or isocyanide all convert Cluster C to the same altered form (C_{red3}, earlier called C*), with an EPR spectrum having all *g* values above 2 (2.28, 2.08, 2.06).[24,26,27] Cyanide, however, converts Cluster C to a different form, having an EPR spectrum with *g* values at 1.87, 1.78, and 1.55.[27,28] The marked sensitivity of the Cluster C EPR spectrum to environment (pH, anions, redox potential) may be attributed to weak electronic coupling ($J < 2$ cm^{-1}) between a high spin Ni(II) site and the $S = {}^1/_2$ state of the $[Fe_4S_4]^{2+/1+}$ cluster.[18]

Cyanide has played an important role in identifying Cluster C as the site of CO oxidation,[17] and in establishing which metals are present,[29,30] because it is a potent inhibitor of CO oxidation activity ($K_i = <10\ \mu M$),[2,29,31,32] but affects acetyl-CO synthesis only at high concentrations.[2,33,34] In this present work, we have used cyanide to characterize Cluster C bonding with resonance Raman (RR) and infrared (IR) spectroscopy. The spectra indicate that cyanide binds simultaneously to the Ni and Fe components of Cluster C in a bent $Fe^{II}-CN-Ni$ bridging geometry. This result leads us to propose a mechanism in which pre-organization of the metal ions by the enzyme promotes CO oxidation by attack of $Ni^{II}-OH^-$ on $Fe^{II}-CO$, followed by Cluster C reduction as CO_2 is released.

Materials and Methods

Growth of the Organism and Enzyme Purification. *C. thermoaceticum* strain ATCC 39073 was grown with glucose as the carbon source at 55 °C as previously described.[35] Isolation and purification of CODH/ACS[2] were performed in a Vacuum Atmospheres (Hawthorne, CA) anaerobic chamber maintained at 14 °C and below 1 ppm of oxygen. Oxygen levels were monitored continuously with a Model 317 trace oxygen analyzer (Teledyne Analytical Instruments, City of Industry, CA). The purified protein was stored in liquid nitrogen. Isotopically labeled protein was prepared in the same manner, but with isotopically enriched metal salts. The metal isotopes were obtained from Advanced Material & Technology (New York). Purified CODH/ACS had an average specific activity of 320 units/mg (1 unit = 1 μmol of CO oxidized/min) at 55 °C and pH 7.6 when assayed for CO oxidation with 10 mM methyl viologen as the electron acceptor.[2] The average specific activity of the CODH/ACS in the isotopic exchange reaction between CO and [1-^{14}C]acetyl-CoA was 224 nmol min^{-1} mg^{-1} at 55 °C (28 nmol min^{-1} mg^{-1} at 25 °C) using 340 μM acetyl-CoA, 1 mM CO (solubility of 1 atm CO), 100 mM pH 5.5 Tris−maleate buffer, and 0.1 mM dithiothreitol. Protein concentrations were determined by the Rose Bengal method.[36]

Preparation of Samples for Vibrational Spectroscopy. After concentrating CODH/ACS to 1.0−1.3 mM in 50 mM Tris−DCl/D_2O buffer at pH 7.6 with an Amicon macrosolute concentrator, 150 μL of enzyme was introduced anaeribically into a Circle cell (Spectra Tech). IR spectroscopy was performed on a FTIR Mattson Galaxy 4020 instrument that was purged with N_2 before and during the experiment. The Circle cell contained a Zn−Se crystal and was maintained under anaerobic conditions. CODH/ACS was incubated in either ^{12}CN (Fisher) or ^{13}CN (Cambridge Isotope Laboratories) for 30 min before pipeting into the Circle cell. Spectra (8000 scans) were recorded for 37.8 min at 4-cm^{-1} resolution at a forward speed of 3.6 cm/s using an MCT detector. Stock solutions of 1.0 M KCN were in 50 mM NaOH or NaOD. The resulting spectrum was subtracted digitally (using First software) from that of a CODH/ACS solution that had not been incubated with CN. The subtraction factor was from 0.98 to 1.02.

Resonance Raman spectra were recorded on CODH/ACS samples (1−1.2 mM) prepared as described above except that the buffer was not deuterated. The final cyanide concentrations were 10 mM unless otherwise stated and prepared from stock solutions (100 mM KCN in 50 mM NaOH). The KCN isotopomers were purchased from Cambridge Isotope Labs. Protein samples were maintained at 77 K in liquid nitrogen during data collection. Spectra were obtained for six different preparations, and the CO oxidation and acetyl-CoA synthesis activities were checked afterwards to ensure that laser irradiation had not degraded the enzyme. A coherent Ar^+ laser (476.5-nm line) at *ca*. 90 mW power was used to probe the sample. Spectra were collected by a Spex triplemate spectrograph equipped with a grating (2400 grooves/mm) and an intensified diode array detector (Princeton Instruments). Six spectra were collected for each sample with an accumulation time of ~40 min for each spectrum.

Results

Metal−Cyanide RR Bands. RR spectra of CODH/ACS in the 300−400-cm^{-1} region contain metal−ligand vibrational bands arising from the metal clusters of the enzyme.[13] When cyanide is added (Figure 1), these bands are altered slightly; the 393- and 381-cm^{-1} bands are now at 390 and 384 cm^{-1}, and the 363-cm^{-1} band develops a low-frequency shoulder.[13] More importantly, two new bands are observed, at 384 (coincident with the 384-cm^{-1} cluster band) and at 342 cm^{-1}, which arise from metal−cyanide vibrations, as revealed by their $^{13}CN^-$ and $C^{15}N^-$ sensitivities (Figure 1). These bands shift down to 379 and 335 cm^{-1} in the $^{13}CN^-$ spectrum and to 380 and 337 cm^{-1} in the $C^{15}N$ spectrum. Because of band overlaps, the $C^{15}N$ frequencies are less certain than the $^{13}CN^-$ frequencies, but the shift pattern is clear.

When the RR spectra are examined for adducts that are enriched in ^{64}Ni or ^{54}Fe, the 342-cm^{-1} band is found to have little metal isotope sensitivity (Figure 2). The 384 cm^{-1} band, however, is seen to shift for both isotopes. In both the ^{12}CN and $^{13}CN^-$ spectra, this band shifts down by 5 cm^{-1} upon ^{64}Ni substitution, and up by 1−2 cm^{-1} upon ^{54}Fe substitution. Because of overlap with the 384-cm^{-1} cluster mode, the ^{54}Fe shift is obscured in the $^{12}CN^-$ spectra, but it is apparent in the $^{13}CN^-$ spectra, where a 380-cm^{-1} shoulder is clearly discernable next to the 384-cm^{-1} cluster band. Also, the $^{13}CN^-$ spectra establish that in the metal isotope spectra there is no remnant intensity at the unshifted position, 378 cm^{-1}, ruling out the possibility that there are two cyanide adducts, one involving Ni and the other involving Fe, which happen to have the same vibrational frequency. The sensitivity of a single vibrational mode to both isotopes means that the CN^- binds to both Ni and Fe, simultaneously.

To gain insight into the origins of the RR bands, we modeled their frequencies and isotope shifts with four-atom normal mode calculations for a variety of bridging geometries, both μ-1,1

(26) Kumar, M.; Lu, W.-P.; Smith, A.; Ragsdale, S. W.; McCracken, J. *J. Am. Chem. Soc.* **1995**, *117*, 2939−2940.
(27) Kumar, M.; Ragsdale, S. W. *J. Am. Chem. Soc.* **1995**, *117*, 11604−11605.
(28) Anderson, M. E.; DeRose, V. J.; Hoffman, B. M.; Lindahl, P. A. *J. Inorg. Biochem.* **1993**, *51*, Abstract B149.
(29) Ensign, S. A.; Hyman, M. R.; Ludden, P. W. *Biochemistry* **1989**, *28*, 4973−4979.
(30) Ensign, S. A.; Bonam, D.; Ludden, P. W. *Biochemistry* **1989**, *28*, 4968.
(31) Morton, T. A. Ph.D. Thesis, University of Georgia, 1991.
(32) Anderson, M. E.; Lindahl, P. A. *Biochemistry* **1994**, *33*, 8702−8711.
(33) Ragsdale, S. W.; Wood, H. G. *J. Biol. Chem.* **1985**, *260*, 3970−3977.
(34) (a) Raybuck, S. A.; Bastian, N. R.; Orme-Johnson, W. H.; Walsh, C. T. *Biochemistry* **1988**, *27*, 7698−7702. (b) Diekert, G.; Hansch, M.; Conrad, R. *Arch. Microbiol.* **1984**, *138*, 224.
(35) Andreesen, J. R.; Schaupp, A.; Neurater, C.; Brown, A.; Ljungdahl, L. G. *J. Bacteriol.* **1973**, *114*, 743−751.
(36) Elliott, J. I.; Brewer, J. M. *Arch. Biochem. Biophys.* **1978**, *190*, 351−357.

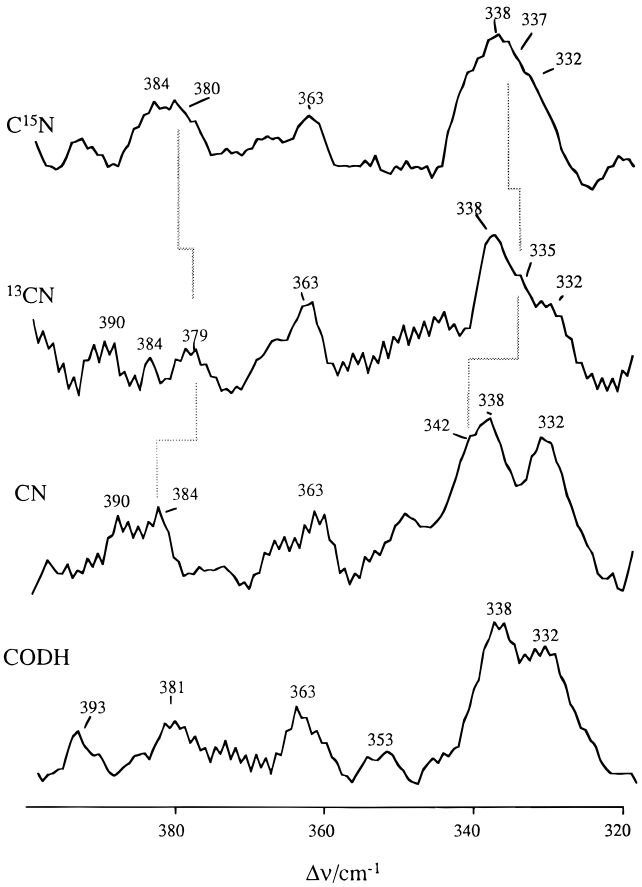

Figure 1. Resonance Raman spectra (476.5 nm Ar^+ laser excitation) in the 320−400-cm^{-1} region. Incubation of CODH/ACS with cyanide induces slight shifts in cluster mode frequencies and produces two new bands, at 342 and 384 cm^{-1}, which are sensitive to the replacement of CN^- with $^{13}CN^-$ and $C^{15}N^-$. As in previous work,[13] a 360 cm^{-1} band buffer has been subtracted digitally.

(both metal atoms bound to the C atom or to the N atom) and μ-1,2 (one metal bound to C and the other to N). It proved impossible to fit the data for a μ-1,1 geometry using a physically reasonable force field. There is, in fact, no precedent for this geometry among the known cyanide bridged complexes, all of which are μ-1,2. Within the μ-1,2 motif, there are a wide range of bond angles, particularly at the N atom. We were unable to model the data satisfactorily with a linear bridge, but obtained a good fit by employing a Fe−CN−Ni complex with all atoms in a plane, and having Fe−C−N and C−N−Ni angles[37] of 175° and 140°.

Such a complex should have six vibrational modes, five in the plane and one out of the plane. The in-plane modes consist of the C−N stretch, an isolated mode near 2100 cm^{-1} (see next section), and four modes below 1000 cm^{-1}, having contributions from Fe−C and Ni−N stretching and Fe−C−N and Ni−N−C bending. Our calculation predicted that, in addition to the modes corresponding to the 384- and 342-cm^{-1} RR bands already observed, the two remaining in-plane modes should be at 80 and 710 cm^{-1}. The former frequency is obscured by background scattering in our spectra, but a careful search of the 700-cm^{-1} region did reveal a band at 719 cm^{-1}, which shifted appropriately upon ^{13}CN and $C^{15}N$ substitution, as seen in Figure 2. This band is weak, and its signal only marginally exceeds the noise, but its detection lends confidence in the validity of the model.

(37) 175° was employed instead of 180° to avoid complications associated with the higher symmetry at exact linearity.

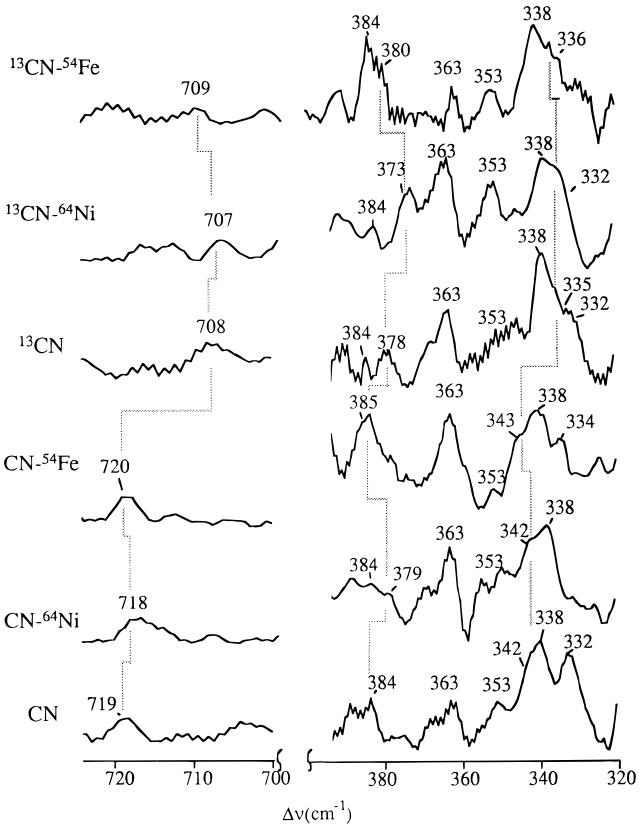

Figure 2. Resonance Raman spectra (conditions as in Figure 1) of the CODH−CN complex, showing metal isotope sensitivity of cyanide-associated bands for natural abundance and ^{13}CN adducts of CODH/ACS, which was isolated from cells grown in medium enriched in ^{54}Fe (98%) and ^{64}Ni (95%).

Table 1. Observed Frequencies and Isotopic Shifts for CN^- Related Modes (cm^{-1})

freq	$\Delta^{15}N$	$\Delta^{13}C$	$\Delta^{64}Ni$	$\Delta^{54}Fe$
342	5	7	0	−1
384	4	5	5	−2
719	12	11	1	−1

The preferred model complex was obtained by carrying out a series of calculations for a Fe−C−N−Ni unit with variable Ni−N−C angle, and also an Ni−C−N−Fe unit with variable Fe−N−C angle. *A priori* it seemed possible that the C end of the CN^- could be bound to either metal (although the CN stretching frequency favors Fe—see next section), and bending is expected to occur at the N end, as was observed, for example, by Scott and Holm[38] in a series of $Fe^{III}-CN-Cu^{II}$ complexes. (In any event, trial calculations with both ends of the bridge bent were unsuccessful.) Force constants were chosen (Table 1) to be physically reasonable, and to bring the frequencies and isotope shifts into optimum agreement with the observed values for the 384- and 342-cm^{-1} bands; the weak 719-cm^{-1} band was not included in the optimizations.

The results of systematically varying the bending angle are shown graphically in Figure 3. The frequencies and isotope shifts all vary strongly with the angle, reflecting changes in the mode composition.[39] When the bridge is linear, the 342- and

(38) Scott, M. J.; Holm, R. H. *J. Am. Chem. Soc.* **1994**, *116*, 11357−11367.

(39) We note that the kinematics of the metal−cyanide vibrations are quite different in the bridged complex than in mononuclear cyanide adducts, for which two modes, M−CN stretching and bending, are found in the 300−450-cm^{-1} region [Simianu, M. C.; Kincaid, J. R. *J. Am. Chem. Soc.* **1995**, *117*, 4628].

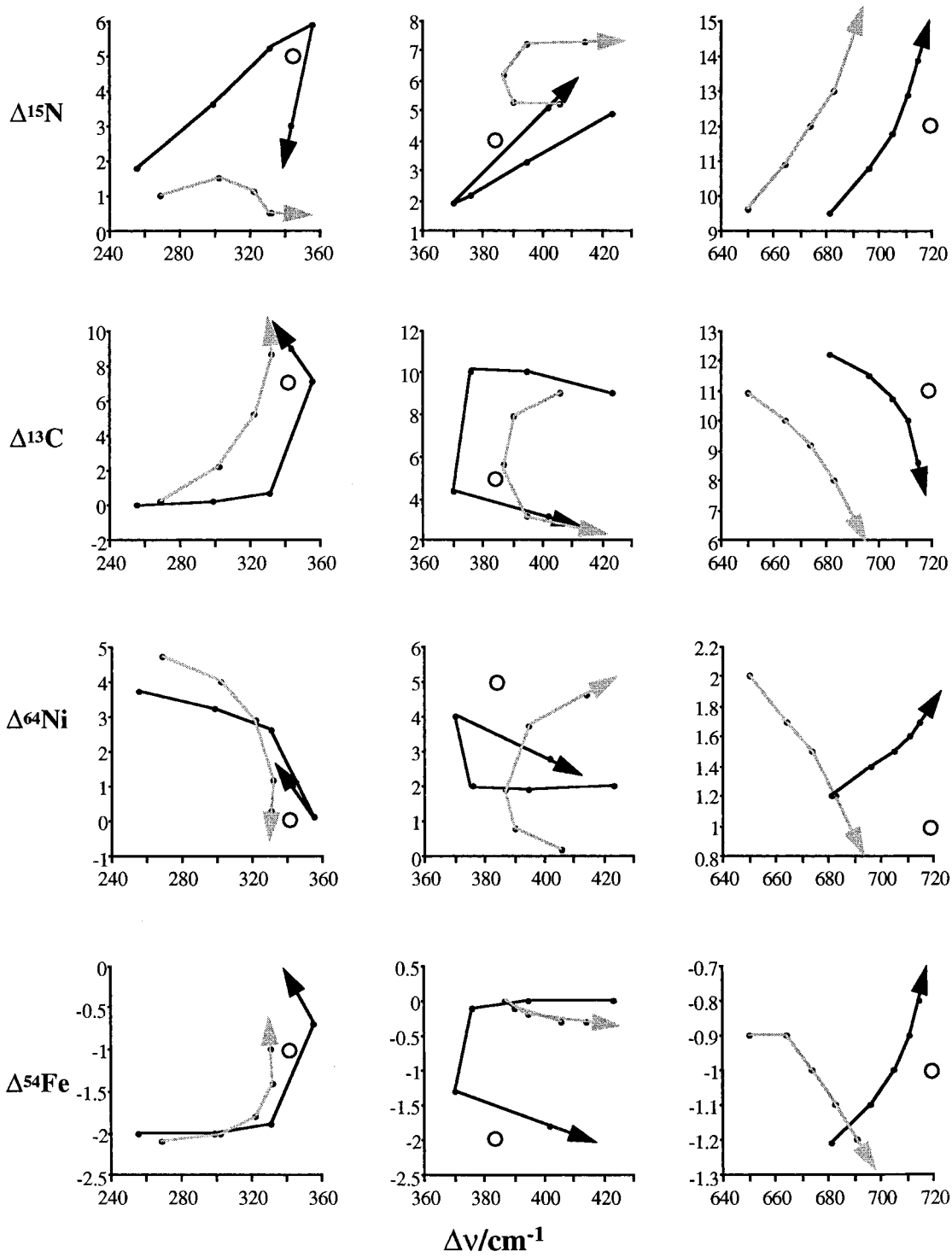

Figure 3. Isotope shift vs frequency plots for the cyanide-associated modes at ~340, ~380, and ~720 cm^{-1}, using a Fe−C−N−Ni (dark line) or Ni−C−N−Fe (light line) model (force constants in Table 1; standard bond distances), with ∠M−C−N = 175° and variable ∠C−N−M′ [values plotted for 175°, 160°, 150°, 140°, 130°]. The arrows indicate the direction of decreasing ∠C−N−M′. The experimental data are plotted as open symbols. The Fe−C−N−Ni model with ∠C−N−Ni = 140° gives the best overall agreement with the data.

719-cm^{-1} modes are the in-phase and out-of-phase metal-ligand stretching modes, while the 384-cm^{-1} mode and the additional mode calculated at 80 cm^{-1} are in-phase and out-of-phase bending modes. As the C−N−metal angle decreases, the stretching and bending coordinates mix, particularly in the 384- and 342-cm^{-1} modes, resulting in a scrambling of the isotope shifts. Consequently, the experimental data discriminate strongly among the test geometries. For example, a linear bridge is immediately ruled out by the ^{13}CN shifts, which are predicted to be zero for the lower frequency (342 cm^{-1}) band and 9 cm^{-1} for the higher frequency (384 cm^{-1}), instead of the observed 7 and 5 cm^{-1}. Likewise the two bands should have large (4−5 cm^{-1}) and small (0−2 cm^{-1}) ^{64}Ni shifts, respectively, for a linear bridge, whereas the observed shifts, 0 and 5 cm^{-1}, are the reverse. The ^{13}CN and ^{64}Ni shifts are close to the values calculated with a 140° bridging angle for either Fe−C−N−Ni or Ni−C−N−Fe.

The alternative metal placements can be distinguished by the ^{54}Fe and ^{15}N shifts. If Fe were bound to N, the 384-cm^{-1} band would show a negligible ^{54}Fe shift and a large (7 cm^{-1}) ^{15}N shift, but this is not observed. Instead, the ^{15}N shift is only 4 cm^{-1}, while a 2-cm^{-1} shift is seen for ^{54}Fe. These values are

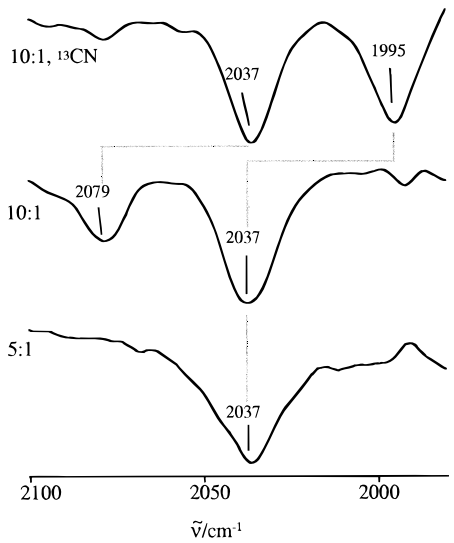

Figure 4. FTIR spectra of the CODH−CN adduct (1.0 mM in 50 mM Tris−DCl/D_2O, pD 7.6) with 5:1 and 10:1 CN^-/CODH molar ratio (showing the appearance of the 2079-cm^{-1} band only at high CN^- concentration), and [top] the 10:1 spectrum for the $^{13}CN^-$ adduct. Protein, buffer, and solvent contributions were subtracted digitally with a reference spectrum of the same solutions without CN^-.

in good agreement with the Fe−C−N−Ni calculation at 140°. This calculation is also in much better agreement with the ^{15}N shift, 5 cm^{-1}, of the 342-cm^{-1} band; the Ni−C−N−Fe model predicts a very small ^{15}N shift, 0−1 cm^{-1}, at any angle. The Fe−C−N−Ni calculation also gives better agreement with the data for the ∼720-cm^{-1} mode, although these were not included in the optimization. The vibrational analysis therefore provides strong support for a model of the Cluster C adduct in which an essentially linear $Fe^{II}CN$ unit interacts with a Ni^{II} ion at an angle of about 140°.[40]

CN Stretching Infrared Band. The IR spectrum of CODH/ACS incubated with cyanide in deuterated buffer (Figure 4) contains bands at 2037 and 2078 cm^{-1}, whose 43-cm^{-1} ^{13}CN isotopic shifts identify them as C−N stretching vibrations, ν_{CN}. These bands are assigned respectively to tight and loose CN^- binding sites on the basis of their CN^- concentration dependence. The 2037-cm^{-1} band could be seen when the cyanide/enzyme molar ratio is as low as two, but the 2078-cm^{-1} band only appeared at ratios greater than five. We infer that the 2037-cm^{-1} band arises from Cluster C, the site of tight cyanide binding,[41] while the 2078-cm^{-1} band reflects some other binding site on enzyme.[42] This weaker adduct is not reflected in the RR spectra, which are the same at low and high cyanide ratios.

The 2037-cm^{-1} Cluster C frequency is exceptionally low. Binding to a metal ion generally raises ν_{CN} from its free ion value, 2078 cm^{-1}, because polarization of the carbon lone pair reduces the C−N antibonding character of the sp σ^* molecular orbital. Only when the metal ion is a strong π donor is the frequency lowered, because of back-donation into the π^* molecular orbital. The Fe^{II}−CN adducts of myoglobin[43a] or of horseradish peroxidase,[43b] for example, have ν_{CN} = 2057 and 2029 cm^{-1}, close to the CODH/ACS value. Ni^{II} is not as effective a π donor as Fe^{II}; the ν_{CN} frequencies[44] in $[K_2Ni(CN)_4]$, for example, range from 2124 to 2144 cm^{-1}, about 100 cm^{-1} higher than the CODH/ACS value.

We note that adding a second metal ion to a cyanide adduct is expected to produce an additional increase in ν_{CN}, because of the added stabilization of the σ^* orbital, but this effect is diminished for bent C−N−M angles. Scott and Holm[38] found that ν_{CN} decreased by 60 cm^{-1} as the C−N−Cu angle in their Fe^{III}−CN−Cu^{II} complexes decreased from 175° to 140°. This difference is comparable to the difference between CODH/ACS (2037 cm^{-1}) and the linear Fe^{II}−CN−Ni^{II} bridge of the Ni[Fe(CN)$_6$] lattice (2114 cm^{-1}).[45] Thus, the 2037-cm^{-1} frequency is consistent with a bent bridge in CODH/ACS and a strongly π-donating metal ion, equivalent to low-spin Fe^{II} in $[Fe(CN)_6]^{4-}$.

Discussion

Cluster C and the Cyanide Adduct. CODH/ACS has the remarkable property of catalyzing CO oxidation and CO incorporation into acetyl-CoA, at separate catalytic centers, both of which contain Ni and a Fe_4S_4 cluster. That Ni and Fe are intimately involved in acetyl synthesis at Cluster A has been evident for some time, thanks to metal isotope line-broadening in the EPR spectrum of the CO adduct.[4,9] The makeup of Cluster C has been more elusive, since CO does not form a stable adduct, but is rapidly oxidized. However, freeze-quench RR spectroscopy has recently provided direct evidence for the involvement of Ni,[13] since the ^{64}Ni-sensitive 365-cm^{-1} band of the enzyme disappears on the time scale (10 ms) of the reduction of Cluster C by CO. The present study supports this involvement by showing ^{64}Ni sensitivity for RR bands associated with bound cyanide, a potent inhibitor of CO oxidation.

Cluster C can be more thoroughly characterized in another CODH, $CODH_{Rr}$ from the photosynthetic bacterium *Rhodospirillium rubrum*, because this enzyme lacks Cluster A, and only catalyzes CO oxidation.[22] The Cluster C EPR and Mössbauer signatures are similar in $CODH_{Rr}$ and CODH/ACS.[18] The Fe EXAFS of $CODH_{Rr}$ is typical for Fe−S clusters, while the Ni EXAFS indicates 2 S donors and 2−3 N/O donors, and is inconsistent with Ni being incorporated into the corner of a Fe−S cluster.[46] $CODH_{Rr}$ can be prepared in an Ni-deficient form, which can be restored to activity by adding Ni.[29,30] The Cluster C EPR and Mössbauer signatures of Ni-deficient $CODH_{Rr}$ are typical for an Fe_4S_4 cluster, but they are significantly altered in the native [or Ni-restored] protein.[18] In the C_{red1} (−300 mV) state of native $CODH_{Rr}$, the Mössbauer spectrum contains a "ferrous component II" signal, similar to that of the substrate binding site of the $[Fe_4S_4]^+$ cluster of aconitase.[47,48] This binding site of aconitase has unique hexacoordinate geometry, although five-coordination is considered likely for the corresponding site in $CODH_{Rr}$,[18] from a

(40) This bonding arrangement contrasts with that of the [4Fe−4S] cluster of a ferredoxin from *Pyrococcus furiosus* where cyanide displaces an aspartate ligand to form an end-on Fe−CN adduct with one of the iron sites in the mixed valent pair [Telser, J.; Smith, E. T.; Adams, M. W. W.; Conover, R. C.; Johnson, M. K.; Hoffman, B. M. *J. Am. Chem. Soc.* **1995**, *117*, 5133].

(41) The inhibition constant of cyanide for the CO oxidation reaction is 3 μM [Morton, T. A. Ph.D. Thesis, University of Georgia, 1991]. Inhibition of acetyl-CoA synthesis requires much higher concentrations of cyanide [Ragsdale, S. W.; Wood, H. G. *J. Biol. Chem.* **1985**, *260*, 3970−3977].

(42) An alternate possibility, that the 2078-cm^{-1} band arose from free cyanide, can be ruled out because the pD of the reaction mixture was maintained between 7.6 and 8.1, where cyanide exists as DCN [pK_a = 9.2], whose C−N stretch is at 1887 cm^{-1} in D_2O [confirmed in control IR spectra].

(43) Reddy, K. S.; Yonetani, T.; Tsuneghige, A.; Chance, B.; Kushkuley, B.; Stavrov, S. S.; Vanderkoii, J. M. *Biochemistry* **1996**, *35*, 5562−5570. (b) Yoshikawa, S.; O'Keeffe, D. H.; Caughey, W. S. *J. Biol. Chem.* **1985**, *260*, 3518−3528.

(44) Kubas, G. J.; Jones, L. H. *Inorg. Chem.* **1974**, *13*, 2816.

(45) Sinha, S.; Humphrey, B. D.; Bocarsly, A. B. *Inorg, Chem.* **1984**, *23*, 203−206.

(46) Tan, G. O.; Ensign, S. A.; Ciurli, S.; Scott, M. J.; Hedman, B.; Holm, R. H.; Ludden, P. W.; Korszun, Z. R.; Stephens, P. J.; Hodgson, K. O. *Proc. Natl. Acad. Sci. U.S.A.* **1992**, *89*, 4427−4431.

(47) Kent, T. A.; Dreyer, J.-L.; Kennedy, M. C.; Huynh, B. H.; Emptage, M. H.; Beinert, H.; Münck, E. *Proc. Natl. Acad. Sci. U.S.A.* **1982**, *79*, 1096−1100.

(48) Beinert, H.; Kennedy, M. C. *Eur. J. Biochem.* **1989**, *186*, 5−15.

comparison of the isomer shift with that of synthetic Fe_4S_4 compounds with one site having FeS_3N_2 coordination.[49−52] Thus, incorporation of Ni in $CODH_{Rr}$ expands the coordination sphere of one Fe^{2+} ion in the Cluster C Fe_4S_4 cluster, creating a binding site for exogenous ligands. A model was suggested[18] in which this Fe^{2+} ion is bridged to Ni^{2+}; weak antiferromagnetic coupling ($J < 2$ cm^{-1}) can explain[18] the unusual EPR spectra induced by azide[26] and thiocyanate[24] binding.

Cyanide binding to $CODH_{Rr}$ perturbs the ferrous component II Mössbauer signal, suggesting that CN^- binds to the five-coordinate site, Fe_A.[18] The low C−N stretching frequency observed in this study, 2037 cm^{-1}, is consistent with Fe^{2+} binding, since substantial π back-donation is indicated; Fe^{2+} is a stronger potential π-donor than Ni^{2+}. Effective π-back-bonding requires that the C atom be bound to the π-donor. Consistent with these considerations, the vibrational modeling is in better agreement with the isotope shift pattern of the RR spectra for a Fe−CN−Ni than a Ni−CN−Fe complex.

When bound to CN^-, Fe^{2+} is normally low-spin, since a short Fe−CN bond is required for effective back-donation. However, a short Fe−CN distance does not necessarily imply spin-pairing in the irregular coordination geometry of the proposed Fe_A site, and indeed the EPR characteristics do not indicate a gross alteration in electronic structure upon CN^- binding.[18] Collectively, the data do support the idea that CN^- binds to Fe_A via its C end in an essentially linear fashion, in order to maximize back-bonding.

The RR data require that the CN^- also be bound to Ni, and vibrational modeling shows the frequencies and isotope shifts to be consistent with a bent bridging geometry, in which the Ni is bound at an angle of about 140° to the end of an essentially linear FeCN unit. This geometry is quite well defined because the vibrational coordinate mixing, and therefore the isotope shift pattern, is strongly dependent on the bridging angle. Also the C−N stretching frequency would be expected to be higher than it is, even considering back-donation from Fe^{2+}, if the bridge to Ni^{2+} were linear, as in $Ni[Fe(CN)_6]$.[45]

The CO Oxidation Mechanism. Does the Cluster C−cyanide adduct have implications for the mechanism of CO oxidation? The strong inhibition by cyanide suggests an affirmative answer, but Anderson and Lindahl[32] proposed that CO and cyanide bind at separate sites because CN^- is a slow-binding inhibitor, and because CO protects against CN^- inhibition and accelerates the dissociation of CN^- from both the *R. rubrum*[29] and *C. thermoaceticum* enzymes.[32] However, these observations are also consistent with a common binding site, but different binding *modes* for the two ligands. Specifically, we suggest that CO, as well as CN^-, binds to Fe_A. The binding of CO depends even more strongly on π back-donation than does CN^- binding, and Fe_A is the only plausible site for effective back-donation. However, CO is unlikely to bind simultaneously to the nearby Ni^{2+}, as CN^- does. Although back-donation enhances the negative charge on both ligands, the charge on bound CO is much less than that on bound CN^-. Consequently, the electrostatic attraction to the positive Ni^{2+} would be lower. The situation bears a resemblance to the distal H-bonding seen in the O_2 adduct of myoglobin[53] but not in the CO adduct.[54] Charge transfer from Fe^{2+} to the ligand is greater for O_2 than CO, with the consequence that a suitably position

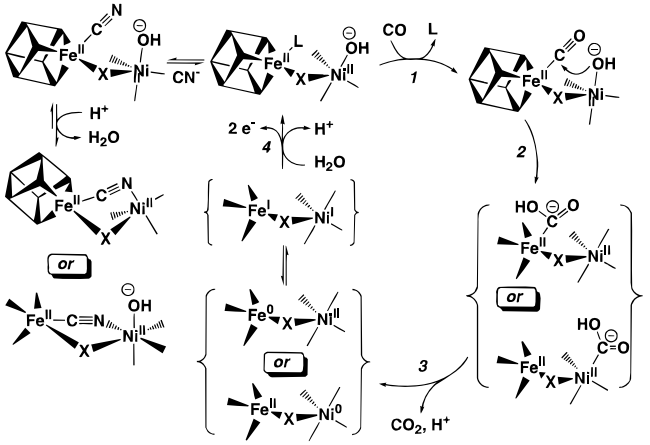

Figure 5. Proposed bimetallic mechanism for CO oxidation. CO binds to Fe^{II} (step 1), and is attacked by Ni^{II}-bound hydroxide, producing a carbohydroxy complex of Fe^{II}, or, alternatively of Ni^{II} (step 2). Internal redox (step 3) releases CO_2 and H^+, transiently forming Fe^0 or Ni^0; the process may be promoted by electron transfer to the Fe^I, Ni^I oxidation level. Electron transfer out of Cluster C (to Cluster B), and release of a proton from Ni^{II}-bound water (step 4), returns the active site to its starting point. CN^- binds to Fe^{II} competitively with CO, and then forms an additional bond to Ni^{II}, thereby increasing the binding constant, and slowing the reversal of CO inhibition.

H-bond donor, the distal histidine, forms an interaction with bound O_2 but not with bound CO.

The additional interaction with Ni^{2+} in the bridged complex can explain the slow inhibition of CO oxidation by CN^-, as illustrated in Figure 5. Initial binding of CN^- to Fe^{2+} would be rapid and reversible by CO; however, a slow subsequent rearrangement to the bridged complex would be more difficult to reverse. CO would nevertheless protect against CN^- inhibition by tying up the Fe^{2+} site. And it could accelerate CN^- dissociation[29,32] by producing a transient mixed complex, with CO bound to Fe^{2+} and CN^- bound to Ni^{2+}.

This model of the inhibited active site provides the basis for a mechanistic proposal regarding CO oxidation (Figure 5). The Fe_A^{2+} ion provides the docking site (step 1) for the CO. The adjacent Ni^{2+} ion does not itself bond to the CO, but is properly positioned to act as a Lewis acid catalyst and to deliver hydroxide for nucleophilic attack (step 2). We note that a similar proposal was recently advanced by Hu et al.,[18] although they suggested hydroxide binding to Fe_A^{2+} and CO binding to Ni^{2+}. A reversal of the roles of the metals is clearly indicated by the present spectroscopic data. Support for the idea of metal-assisted hydroxide attack comes from the pK_a of 7.5 for the CO oxidation activity pH profile.[24] This is a reasonable value for ionization of a water molecule that is coordinated to a buried Ni^{II} ion.

A precedent for Ni^{II}-assisted hydroxide attack on a carbonyl compound at a bimetallic center exists in the enzyme urease.[55,56] No redox chemistry ensues in urease, the overall reaction being urea hydrolysis. In the CODH mechanism, however, hydroxide attack (step 2) produces bound carbohydroxy ion, $^-$COOH, a strong reductant.[57] It can release CO_2 and H^+ by transferring an electron pair to the Fe^{II} (step 3). Alternatively, the hydroxide

(49) Ciurli, S.; Carrié, M.; Weigel, J. A.; Carney, M. J.; Stack, T. D. P.; Papaefthymiou, G. C.; Holm, R. H. *J. Am. Chem. Soc.* **1990**, *112*, 2654−2664.

(50) Ciurli, S.; Yu, S.-B.; Holm, R. H.; Srivastava, K. K. P.; Münck, E. *J. Am. Chem. Soc.* **1990**, *112*, xxxx.

(51) Ciurli, S.; Ross, P. K.; Scott, M. J.; Yu, S.-B.; Holm, R. H. *J. Am. Chem. Soc.* **1992**, *114*, 5415−5423.

(52) Zhou, J.; Scott, M. J.; Hu, Z.; Peng, G.; Münck, E.; Holm, R. H. *J. Am. Chem. Soc.* **1992**, *114*, 10843−10854.

(53) Phillips, S. E. V.; Schoenborn, B. P. *Nature (London)* **1981**, *292*, 81−82.

(54) Hanson, J. C.; Schoenborn, B. P. *J. Mol. Biol.* **1981**, *153*, 117−146.

(55) Blakeley, R. L.; Zerner, B. *J. Mol. Catal.* **1984**, *23*, 263−292.

(56) Jabri, E.; Carr, M. B.; Hausinger, R. P.; Karplus, P. A. *Science* **1995**, *268*, 998−1004.

(57) Collman, J. P.; Hegedus, L. S.; Norton, J. R.; Finke, R. G. In *Principles and Applications of Organometallic Chemistry*; University Science Books: Mill Valley, CA 1987; pp 403−620.

attack could be accompanied by attachment of $^{-}$COOH to Ni^{II}, instead of Fe^{II}. This step might be energetically advantageous, since Ni^{II} is generally easier to reduce than is Fe^{II}. In either case, the two-electron oxidation requires generation of zero-valent metal, Fe[0] or Ni[0], either in the transition state or as a transient intermediate. This high-energy step can be assisted, however, by rapid electron transfer to the neighboring metal, forming a Fe^{I},Ni^{I} center. This reduced form of Cluster C would then deliver two electrons (step 4), via Cluster B, to Cluster A, where they are utilized in acetyl-CoA synthesis.[12]

If this mechanistic proposal is correct, then there is a striking parallel between the chemistries of CO oxidation and of acetyl-CoA synthesis in CODH/ACS. Both utilize a Ni atom to facilitate attack on Fe-bound CO.[58] At Cluster C, the attacking group is a hydroxide nucleophile, while at cluster A, the attacking group is a methyl electrophile.[59] In both centers, the structural motif appears to be a Ni atom bridged to a Fe_4S_4 cluster, at a Fe^{2+} ion with an available coordination site. We speculate that the difference in chemistry resides in the Ni coordination environment, which favors Ni^{2+} at Cluster C, but low-valent Ni at Cluster A, in order to facilitate OH^{-} transfer at the former and CH_3^{+} transfer at the latter.

In CODH/ACS, Nature has anticipated industrial chemistry, which also utilizes transition metal based catalysts for CO oxidation and reduction processes. The synthesis of acetyl-coenzyme A at Cluster A is analogous to industrial acetic acid synthesis by methylation of CO,[60,61] while the oxidation of CO at Cluster C is analogous to the water gas shift reaction,[57] a source of industrial hydrogen: $CO + H_2O = CO_2 + H_2$. The industrial catalysts are not, however, pre-organized to juxtapose different metal atoms, as CODH/ACS is. This may explain why the industrial processes require elevated temperatures and pressures, whereas CODH/ACS does not.

Acknowledgment. This work was supported by NIH grants GM 13498 (to T.G.S.) and GM 39451 (to S.W.R.).

JA960435F

(58) Qiu, D.; Kumar, M.; Ragsdale, S. W.; Spiro, T. G. *Science* **1994**, *264*, 817−819.
(59) Kumar, M.; Qiu, D.; Spiro, T. G.; Ragsdale, S. W. *Science* **1995**, *270*, 628−630.
(60) Forster, D. J. *J. Am. Chem. Soc.* **1976**, *98*, 846−848.
(61) Forster, D. J. *Adv. Organomet. Chem.* **1979**, *17*, 255−266.